



Continuum modeling of the cohesive energy for the interfaces between films, spheres, coats and substrates



Junhua Zhao^{a,b,*}, Lixin Lu^a, Zhiliang Zhang^c, Wanlin Guo^d, Timon Rabczuk^{b,*}

^aJiangsu Key Laboratory of Advanced Food Manufacturing Equipment and Technology, Jiangnan University, 214122 Wuxi, China

^bInstitute of Structural Mechanics, Bauhaus-University Weimar, 99423 Weimar, Germany

^cDepartment of Structural Engineering, Norwegian University of Science and Technology (NTNU), 7491 Trondheim, Norway

^dState Key Laboratory of Mechanics and Control of Mechanical Structures, Nanjing University of Aeronautics and Astronautics, 210016 Nanjing, PR China

ARTICLE INFO

Article history:

Received 11 February 2014

Received in revised form 11 June 2014

Accepted 23 June 2014

Available online 21 July 2014

Keywords:

Cohesive energy

Thin film

Sphere

Matrix

Substrate

Continuum model

ABSTRACT

Explicit solutions of the cohesive energy for the interfaces between film/coat, sphere/coat, sphere/matrix and sphere/substrate are obtained by continuum modeling of the van der Waals interaction between them. The analytical results show that the cohesive energy strongly depends on their size and spacing. For a given film thickness and sphere radius, the cohesive strength increases with increasing coat thickness and then tends to a constant when the coat thickness is up to a critical value. The cohesive strength for the interface between sphere/matrix keeps a constant when the sphere radius is up to a critical value. Checking against full atom molecular mechanics calculations show that the continuum solution has high accuracy. The established analytical solutions should be of great help for understanding the interactions between the nanostructures and substrates, biomaterials, designing nanocomposites and nanoelectromechanical systems.

© 2014 Elsevier B.V. All rights reserved.

1. Introduction

The interfaces between various micro/nanoscale structures strongly affect the physical, chemical and mechanical properties of the structures. A fundamental understanding of the interface strength is of major importance in nanoelectromechanical devices, biomaterials, microelectronics and microsystems. The physical and mechanical properties of a biological material are determined not only by its chemical compositions but also by its structures at multiple length scales, which have been selected according to the basic rules of evolution and optimization in nature. Nacre is composed of more than 95% (by volume) mineral content of CaCO_3 and less than 5% soft organic ingredient in form of hierarchical structural architecture extending over several distinct length scales [1–3]. The thickness of the aragonite platelets and the organic interlayers is in the range of 0.2–0.9 μm and 10–45 nm [4], respectively (see Fig. 1a). The aragonite layers usually do not bond well to organic such that their interaction is the van der Waals (vdW) force [1,4]. Shao et al. [5] explained the range of the platelets thickness by a

microstructure-based fracture mechanics model. Dutta et al. [6] studied the mechanical behavior of nacre under impact loading. However, the reason why the organic interlayer thickness is in the range of 10–45 nm still not clear.

In recent years, there has been a renewed interest in using the metalized polymer particles for applications in manufacturing of microelectronics and microsystems [7–9]. One promising application of the polymer spheres has been the development and manufacturing of ultra-thin Liquid Crystal Display (LCD) by means of Anisotropic Conductive Adhesives (ACA) technology (see Fig. 1b) [9,10]. This ACA technology can contribute with reduced package size, lower assembly temperature, and possibly lower cost in the electronic device manufacturing, while the sphere sizes mostly range from 0.1 to 100 μm in diameter for the applications [11,12]. The vdW interactions determine the interface strength between the metal coats and the polymer spheres. The coats thicknesses of the spheres are usually in the range of 10–25 nm in the experiments [13] and the mechanism is also not clear yet.

Recently, the thermal conductivity of the matrix-embedded semiconductor nanocrystals has been reported by experiment [14]. The results show that the ratio of the sphere radius to the coat thickness strongly affects the thermal conductivity [14]. Moreover, the size-selected monodisperse nanoclusters on supported graphene have been systematically studied by experiment [15]. As mechanical structures enter the micro/nanoscale regime, the

* Corresponding authors. Address: Jiangsu Key Laboratory of Advanced Food Manufacturing Equipment and Technology, Jiangnan University, 214122 Wuxi, China (J. Zhao). Tel.: +86 510 85910562 (J. Zhao), +49 3643 584511 (T. Rabczuk).

E-mail addresses: junhua.zhao@163.com (J. Zhao), timon.rabczuk@uni-weimar.de (T. Rabczuk).

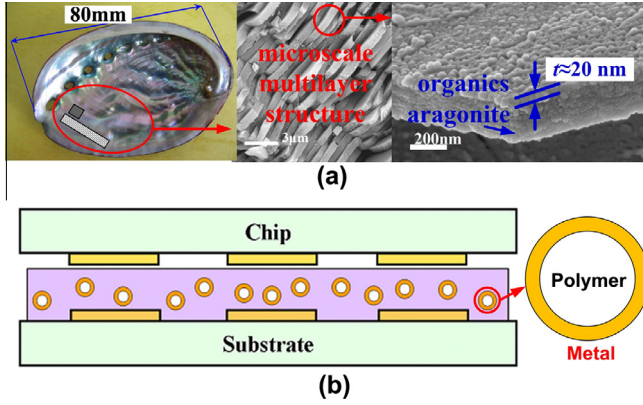


Fig. 1. Schematic plot of nacre and flip-chip connection using anisotropic conductive adhesives (ACA). (a) The optical picture of *Haliotis discus hannai* shell and its scanning electron microscopy images of the micro/nanoscale multilayer structures as well as an individual aragonite platelet with organics; and (b) ACA technology and the coated sphere.

influence of vdW forces plays a significant role [15–21]. Therefore, the vdW interactions between the nanoclusters and graphene have a great effect on these properties. A good understanding of the vdW interactions for the interfaces of the coated film, coated sphere, sphere/matrix, and sphere/substrate is of major importance for their practical applications in the microelectromechanical systems.

In this paper, we obtain the closed-form expressions of the cohesive energy for the interfaces between film/coat, sphere/coat, sphere/matrix and sphere/substrate from a continuum model based on the Lennard-Jones (LJ) potential. Checking against full atom molecular mechanics (MM) calculations show that the continuum solution has high accuracy. The obtained analytical solutions should be of great help for understanding the interaction between the nanostructures and the substrates as well as the biomaterials.

2. Molecular mechanics simulation

To validate the continuum model for two parallel thin films and sphere/substrate, the two different finite-thickness diamond plates and the diamond sphere/plate are built in our MM simulations. Unlike molecular dynamics (MD) simulations, MM simulations don't consider the temperature effect. All the MM simulations are performed using LAMMPS [22] with the AIREBO potential [23]. Note that the two thin films or sphere/substrate are taken as two groups. The AIREBO potential are used in the atoms of the two groups, respectively. The independent LJ potential are used to describe the interactions between the atoms in the two groups. It should be noted that the chosen LJ cutoff radius has a remarkable effect on the accuracy of present results when the LJ cutoff radius is smaller than 15 Å, and then the effect decreases with increasing cutoff radius [24]. In this paper, the LJ cutoff radius is chosen as 40 Å to avoid the effect of the cutoff radius [24]. For the two thin films, we choose the length, width and thickness $L \times W \times t$ as $7.12 \times 7.12 \times 1.068 \text{ nm}^3$ and $7.12 \times 7.12 \times 1.424 \text{ nm}^3$, while the length and width $L \times W$ as $14.5 \times 14.5 \text{ nm}^2$ for two graphene sheets are built to compare with our analytical model (see the inset of Fig. 2). The periodic boundary is applied along the length and width directions, respectively. The free boundary is applied along the thickness direction. For sphere/substrate, the diameter of 1.424 nm with 1.068 nm thickness plates and 3.56 nm diamond sphere with 1.068 nm thickness plate are built to compare with our analytical model, respectively (see the figure in Section 3.3). The diameter of 3.56 nm diamond sphere with

graphene ($L \times W$ is $14.5 \times 14.5 \text{ nm}^2$) are built to compare with our analytical model (see the figure in Section 3.3).

There are three steps to calculate the cohesive energy. First, two parts are kept at a distance of 40 Å, and then relaxed independently. Second, these two sheets are assumed as two rigid bodies and are moved toward each other with small displacement increment. Third, the structure is optimized for each displacement increment and the optimized structure is taken as the initial geometry for the next calculations. The two parts closely move 0.1 Å each other at each time step based on the deformation-control method, respectively. The conjugate-gradient algorithm is applied for the energy minimization, where energy and force tolerances are both equal to 10^{-8} [22].

3. Cohesive energy for the interfaces of the coated thin film, coated sphere, sphere/matrix and sphere/substrate

3.1. A coated thin film

In the context of this paper, the energy of the vdW interactions [22,25] is given by

$$V(d) = 4 \in \left[\left(\frac{\sigma}{d} \right)^{12} - \left(\frac{\sigma}{d} \right)^6 \right], \quad (1)$$

where d is the distance between the interacting atoms, \in is the depth of the potential, σ is a parameter that is determined by the equilibrium distance. In this paper, $\in = 2.8437 \text{ meV}$ and $\sigma = 3.4 \text{ Å}$ are chosen [25,26].

First, we provide a continuum model to establish the analytical expression of the cohesive energy for the interface of the coated thin film, as shown in Fig. 2a. We homogenize the atoms on the coat and film as well as represent them by the volume density ρ_c and ρ_f , where ρ_c and ρ_f are related to the number of atoms per unit volume in the coat and film prior to deformation, respectively [19,20,27]. The coat and the thin film are parallel with each other, and h denotes the distance between them, as shown in Fig. 2a.

The distance between the point A (x_f, z) ($-(h+l) \leq x_f \leq -h$, $z \geq 0$) on the lower film and B ($x_c, 0$) ($0 \leq x_c \leq H$) on the upper coat is $d = ((x_c - x_f)^2 + z^2)^{1/2}$. The cohesive energy ϕ per unit area can be given as

$$\phi = 2\pi\rho_c\rho_f \int_{-(h+l)}^{-h} V(d)dx_f \int_0^\infty zdz \int_0^H dx_c, \quad (2)$$

where H and l are the thickness of coat and film, respectively.

Substituting Eq. (1) into Eq. (2) gives

$$\phi = \frac{1}{3} \pi \rho_c \rho_f \in \sigma^6 \left(\frac{\sigma^6}{30} \left[\left(\frac{1}{h^8} - \frac{1}{(H+h)^8} \right) - \left(\frac{1}{(h+l)^8} - \frac{1}{(H+(h+l))^8} \right) \right] - \left[\left(\frac{1}{h^2} - \frac{1}{(H+h)^2} \right) - \left(\frac{1}{(h+l)^2} - \frac{1}{[H+(h+l)]^2} \right) \right] \right). \quad (3)$$

When $l=H=0$, the cohesive energy ϕ per unit area can be expressed as

$$\phi = 4\pi\rho_c\rho_f \in \sigma^6 \left(\frac{\sigma^6}{5h^{10}} - \frac{1}{2h^4} \right). \quad (4)$$

Assuming the two graphene sheets, then $\rho_c = \rho_f = \rho = 0.3818 \text{ Å}^{-2}$ are the lower and upper area densities of graphene [19].

When $l=0, H=\infty$, the cohesive energy ϕ per unit area can be given as

$$\phi = \frac{2\pi}{3} \rho_c \rho_f \in \sigma^6 \left(\frac{2\sigma^6}{15h^9} - \frac{1}{h^3} \right). \quad (5)$$

Eq. (5) is the same with the results in previous work [20].

Download English Version:

<https://daneshyari.com/en/article/1560481>

Download Persian Version:

<https://daneshyari.com/article/1560481>

[Daneshyari.com](https://daneshyari.com)